

Sloshing cold fronts in the IC1860 group

F. Gastaldello¹, L. Di Gesu^{1,2}, S. Ghizzardi¹, S. Giacintucci³, M. Girardi⁴, E. Roediger⁵, M. Rossetti^{1,2}

¹INAF-IASF Milan, ²Università di Milano, ³University of Maryland, ⁴Università di Trieste, ⁵Jacobs University Bremen

Abstract

We present a combined X-ray, optical, and radio analysis of the galaxy group IC 1860 using the currently available Chandra and XMM data, literature multi-object spectroscopy data and GMRT data. The Chandra and XMM imaging and spectroscopy reveal two surface brightness discontinuities at 45 and 76 kpc shown to be consistent with a pair of cold fronts. We find evidence of a characteristic spiral pattern in the X-ray gas distribution, tilted with respect to the plane of the sky, indicative of a mainly line-of-sight off-axis merger responsible of the sloshing. We identify the likely perturber as an optically disturbed spiral galaxy, IC 1859. The peculiar velocity of the BCG with respect to the mean group velocity is another signature consistent with the sloshing scenario.

The GMRT observation at 325 MHz shows extended radio emission: one component is contained within the inner cold front as seen in some galaxy clusters, whereas the second component is detached and in the vicinity of the spiral feature. The limits obtained from the NVSS at 1.4 GHz points to a very steep spectral emission coming from aged radio plasma.

The analogy with two other groups, NGC 5044 and NGC 5846, showing cold fronts is tantalizing also for the presence of optically disturbed spiral galaxies identified as possible perturbers. X-ray cold fronts witness the influence of the group tidal field on these disk galaxies.

1 Introduction

Chandra and XMM, have revealed a wealth of small scale features in the intra-cluster and intra-group medium (IGM). Particularly interesting are the "cold fronts", sharp surface brightness discontinuities, interpreted as contact edges between regions of gas with different entropies (see the review by Markevitch & Vikhlinin 2007). Cold fronts appear to be ubiquitous in galaxy clusters (e.g., Ghizzardi et al. 2010) and they are found both in merging clusters and in cool core relaxed clusters.

In relaxed clusters cold fronts are most likely induced by minor off-axis mergers that produce a disturbance on the gas in the core of the main cluster, displace it from the center of the potential well, and decouple it from the underlying dark matter halo through ram pressure. The oscillation of the gas of the core around the minimum of the potential generates a succession of radially propagating cold fronts, appearing as concentric edges in the surface brightness distribution of the cluster. These fronts may form a spiral structure when the sloshing direction is near the plane of the sky and the merger has a non-zero angular momentum. When the sloshing direction is not in the plane of the sky concentric arcs are observed (Ascasibar & Markevitch 2006, AM06 hereafter; Roediger et al. 2011, R11 hereafter). Another observable effect is presence of a peculiar velocity of the central galaxy, if it sits at the cusp of the dark matter (DM) distribution and therefore starts oscillating with the DM peak after each subcluster flyby (AM06).

A number of relaxed, cool core clusters are hosts to faint, diffuse radio emission with a radius comparable to the size of the cool core and with a steep spectrum. These sources are called mini radio-halos and they are relatively rare, with only few clusters with confirmed detections (Ferrari et al. 2008 for a review). The sloshing motions can produce turbulence in the cluster core. Mazzotta & Giacintucci (2008) discovered spatial correlations between mini radio-halos emission and cold fronts in the X-ray images of two clusters, with the mini-halos contained within the region confined by the cold fronts and they suggested that the correlation arises from the turbulence generated by the sloshing motions. ZuHone et al. (2012) tested the hypothesis with high resolution MHD simulations of gas sloshing confirming that re-acceleration of relativistic electron seeds (e.g., from past AGN activity) can produce radio mini-halo emission within the envelope of the sloshing cold fronts.

Sloshing cold fronts have been detected also at the smaller mass scales of groups of galaxies (e.g., Gastaldello et al. 2009, G09 hereafter). At this mass scale even a single massive galaxy can be the responsible perturber and the X-ray signature of sloshing cold front is a signature of the gravitational interaction between the galaxy (and its DM halo) and its host group. Here we present the results of the available Chandra and XMM data, optical and radio GMRT data for the IC 1860 group, a nearby group of galaxies at $z=0.022$.

2 XMM and Chandra observations of IC 1860

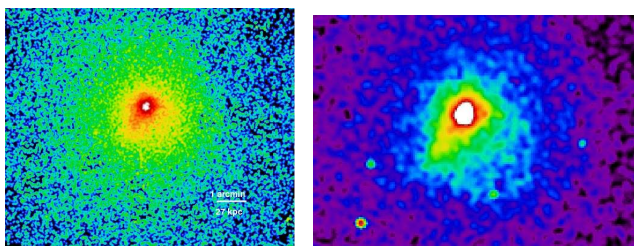


Fig.1 Left panel: exposure corrected mosaic of the MOS1 and MOS2 images in the 0.5-2 keV band smoothed on a 3'' scale. Right Panel: Chandra ACIS-S exposure-corrected image in the 0.7-2 keV band smoothed on a 1.5'' scale.

The XMM and Chandra images in Fig.1 reveal the presence of a brightness discontinuity in the NW and a surface brightness extension from the core to the SE which also ends in a surface brightness discontinuity. A more detailed view is provided by the surface brightness profiles extracted in angular sectors in Fig.2 together with the surface brightness residual map between the XMM data and the best fit one-dimensional β -model. A characteristic spiral pattern is seen as a surface brightness excess even though the qualitative impression is that the overall morphology is tilted with respect to the plane of the sky, with the head of the mushroom structure seen in many hydrodynamic simulations (AM06) pointing towards the observer.

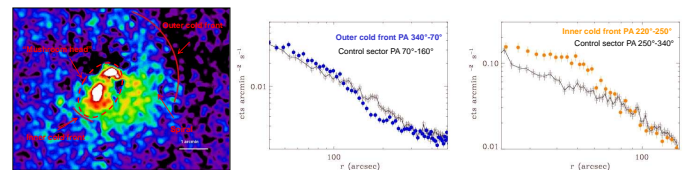


Fig.2 Left panel: Map of the residuals between the XMM image of Fig.1 and the best fit β -model for the data. The center of IC 1860 is shown by the black cross and the position and extent of the cold fronts by the red arcs. Central panel: XMM surface brightness profiles in two sectors, one including the outer cold front and one shown for comparison. PA are measured from the W direction. Right Panel: Chandra surface brightness profiles in two sectors, one including the inner cold front and one shown for comparison.

In Fig.3 we present the results of the XMM spectral fits (Chandra gives consistent results) in the radial bins inside and outside the edges. For the inner edge a clear temperature increase across the edge is detected, as expected for a cold front; there is no statistically significant change in temperature across the outer edge. However taking into account projection effects the picture is consistent with cooler gas inside the edge; a similar behavior has been seen for the outer cold fronts in NGC 5044 (G09) and NGC 5846 (Machacek et al. 2011, M11 hereafter). The emission in the SE leading to the inner cold front is cooler than the surroundings.

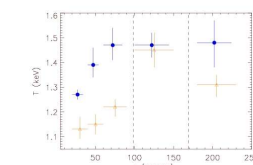


Fig.3 XMM temperature profiles along the sectors containing the cold fronts. The vertical dashed lines mark the position of the inner and outer cold fronts. Orange triangles refer to the 220°-250° sector hosting the inner cold front, blue points the 340°-70° sector hosting the outer cold front.

3 Radio and optical data

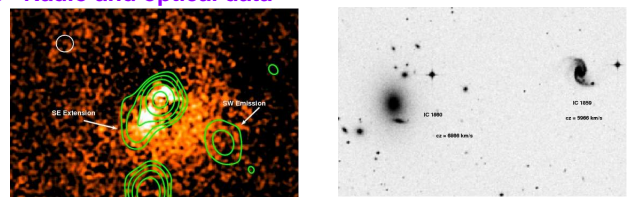


Fig.4 Left panel: GMRT radio contours at 325 MHz overlaid on the map of residuals of Fig.2. The restoring beam is indicated by the white ellipse. The rms noise level is 0.6 mJy beam⁻¹. Contours are spaced by a factor of 2 starting from 2 mJy beam⁻¹. The emission which can be seen in the South is coincident with an X-ray point source. Right Panel: DSS image of the central region of the IC 1860 group.

The GMRT radio image at 325 MHz reveals an extended feature which originates at the IC1860 center and extends from the center towards SE. This radio emission is confined within the inner cold front and traces the "mushroom head" feature interpreted as the tip of the sloshing spiral. A second patch of faint radio emission is visible 2 arcmin SW of the central source. Neither of these extended features are visible in the 1.4 GHz VLA image by Dunn et al. (2010), indicating very steep spectral indexes for these features. The radio emission comes probably from aged radio plasma, perhaps associated with a past episode of activity of the central radio galaxy. In the optical band we collected galaxies with known velocity within 1.6 Mpc of IC 1860. The primary source of these velocities is 2dF (Colless et al. 2003). After exclusion of interlopers the final group sample contains 74 members. The mean group velocity is 6753 ± 44 km/s with a dispersion velocity of 401 ± 46 km/s. The peculiar velocity of the central galaxy IC 1860 with respect to the group mean is 113 km/s significant at the 2.3σ level. We identified as the possible perturber IC 1859, a Seyfert 2 galaxy with a peculiar optical morphology showing a pair of spurs in the eastern spiral arm. It is at a projected distance of 176 kpc from IC 1860 and it has a velocity difference of -880 ± 67 km/s with respect to IC 1860 and of -767 ± 78 km/s with respect to the group mean velocity.

4 Comparison with other groups with sloshing cold fronts

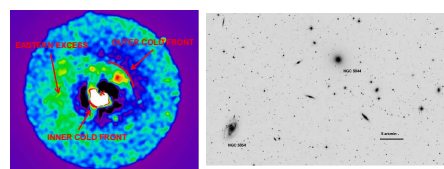


Fig.5 Left panel: Surface brightness residual map for the 0.5-2 keV MOS image of the NGC 5044 group. Central panel: DSS image of the central region of the NGC 5044 group. Right Panel: zoomed DSS image of the galaxy NGC 5054, together with the companion N134.

The analogy of the IC 1860 group with other groups showing cold fronts is tantalizing. For example in the nearby ($z=0.009$) NGC 5044 group where sloshing cold fronts were reported in G09, we show the presence of a large scale brightness excess predicted by sloshing simulations (e.g., R11) which strengthens an earlier suggestion by David et al. (2009) of the identification of the perturber with the disturbed spiral NGC 5054 (see Fig.5). The central galaxy NGC 5044 has a peculiar velocity of 156 km/s with respect to the mean group velocity, significant at the 4.8σ level. A similar situation holds for the NGC 5846 group (M11) with the rich, barred spiral NGC 5850 identified as the perturber (M11).

References

Ascasibar & Markevitch 2006, ApJ, 650, 102 (AM06)
 Colless et al. 2003, astro-ph/0306581
 David et al. 2009, ApJ, 705, 624
 Dunn et al. 2010, MNRAS, 404, 180
 Ferrari et al. 2008, Space Sci. Rev., 134, 93
 Gastaldello et al. 2009, ApJ, 698, 43 (G09)
 Ghizzardi et al. 2010, A&A, 516, A32
 Machacek et al. 2011, ApJ, 743, 11 (M11)
 Markevitch & Vikhlinin 2007, Phys. Rep., 443, 1
 Mazzotta & Giacintucci 2008, ApJ, 675, L9
 Roediger et al. 2011, MNRAS, 413, 2057 (R11)
 ZuHone et al. 2012, arXiv:1203.2994